An in-situ FTIR study of undoped PolyBenzoImadazole as a function of humidity and temperature

P. A. Christensen and S. W. M. Jones
School of Chemical Engineering and Advanced Materials, Bedson Bulding, Newcastle University, Newcastle upon Tyne, NE1 7RU, England, UK.

Abstract

Undoped, cast films of PolyBenzoImadazole (PBI) were investigated as a function of humidity using both H_2O and D_2O, and as a function of temperature up to 100 °C in order to better understand the infrared response of this polymer, as well as to provide benchmark data for subsequent studies on acid doped PBI. Marked changes across the mid-IR range were observed during the uptake of water and D_2O. The use of D_2O proved extremely useful in terms of deconvoluting the complex IR response observed and allowed the IR data to be rationalised in terms of the disruption of the N-H…N inter-chain hydrogen bonded network and changes in the morphology of the polymer.

Introduction

Polybenzimidazole (PBI) is considered as a promising membrane material for High Temperature Polymer-Electrolyte Membrane Fuel Cells (HT-PEMFCs) due to its excellent thermal and chemical stability [1-5], mechanical robustness and high tolerance to CO [6]. PBI has a glass transition temperature of 420 °C and is generally believed to be completely amorphous[7]. The conductivity of the polymer is strongly dependent upon doping with strong acid and can reach 0.25 S cm^{-1} at 180 °C[5].

It is generally believed that there is significant hydrogen bonding between the chains of undoped PBI[8][9][10], see scheme 1. Thus, Ramondo et al [11] studied the effect of intermolecular hydrogen bonding on the structure of imidazole. They found that the N…..H separation is unusually short (ca. 2.86 Å compared with ca. 3.21-3.29 Å in *p*-diaminobenzene for example), and hence particularly strong for such a hydrogen bond. This is supported by the high boiling point of imidazole (256 ^oC) and high degree of its association in non-polar solvents [12]. Scheme 2 shows the two canonical forms of imidazole described by Ramondo and co-workers as the principal contributors to the electronic structure of the molecule. They postulated that hydrogen bonding is associated with an increased contribution of state (II) with respect to state (I) and that

the former is a better proton donor and acceptor than the latter. Furthermore, the authors stated that an increased contribution from (II) leads to a stronger N-H….N interaction, thus explaining the unusually short hydrogen bonds in crystalline imidazole polymers. From their ab initio molecular orbital modelling, Ramondo and co-workers calculated a lengthening of the N_1-H bond upon hydrogen bonding. They also predicted changes in the bonds within the heterocyclic ring, stating that an increase in hydrogen bond strength leads to the shortening of the N_1-C_2 bond by ca. 0.03 Å, and a complimentary increase in the length of C_2-N_3 bond. Hence, when exposed to water vapour, if the uptake of water by PBI does result in the disruption of the inter-chain hydrogen bonds and the formation of hydrogen bonds to water, as shown in scheme 3, this would be expected to have a significant effect upon the IR response of the polymer.

Zielinski and co-workers [13] observed pressure-induced phase transitions in their study of the hydrogen bonding in compressed benzimidazole polymorphs, with the NH….N bonded chains extending along the [011] and [$0\bar{1}1$] lattice planes in phase (α) and along [100] in phases (β) and (γ). Furthermore, they state that in phase (α), the planes of neighbouring molecules are rotated about the direction of the chain as opposed to phases (β) and (γ), within which molecules are rotated perpendicular to the chain. The consequence of this with respect to our work discussed below is that these phase transitions affect the dimensions and energy of the NH….N bond, with Zielinski and co-workers stating that the shortest and hence strongest of these bonds have angles closest to 180^o. Thus, the strength of the NH….N interactions are strongly dependent on the orientation of the H-accepting molecule in the hydrogen bond, the orientation of adjacent PBI chains and hence the structure and morphology of the PBI.

There are a number of IR studies of PBI as a function of doping[7][14 – 16], blend composition [5][8-9][17 – 19] and temperature[5][8][14], and investigating hydrogen bonding in the polymer[8][9][10]. However, with one exception[9], spectral subtraction was not employed and hence small changes in spectral response due to, for example, increasing temperature could not be elucidated. In the work by Musto and colleagues[9] spectral subtraction was employed, but only over the spectral range covering the N-H absorptions of PBI. In fact, discussion of the IR spectra of PBI has largely been confined to the latter region due to the simplicity of the absorptions[14][19] which have, as a consequence, been fully assigned.

Despite the significant number of studies on the IR response of PBI under various conditions, there are none to our knowledge seeking to study the absorptions in the fingerprint region of the polymer. Hence, the aim of this paper is to study the effect of temperature and humidity on the mid-IR spectrum of undoped PBI using in-situ difference spectroscopy to provide benchmark spectral data.

Experimental

Ti discs of 0.95 cm^2 were coated in PBI (Between Lizenz GmbH, Germany, > 99%) by casting from dimethylacetamide (DMAc) and allowed to dry at room temperature for ca. 24h. The PBI was dissolved in the DMAc in a PTFE digestion vessel using microwave heating to a concentration typically of 5-10 wt%. Thus, ca. 0.1 cm^3 PBI/DMAc was placed on the Ti disc using a pipette and allowed to dry. The mass of PBI was then calculated from the mass of the disc and disc+dry film. The density of the dry PBI was taken as 1.3 g cm^{-3} [20] and the loading of dry film calculated accordingly. Four films were so prepared: PBI1 was 4.4 μm thick, whilst PBI2 – 4 were all 7.9 μm thick. PBI 3 and 4 were prepared simply as duplicates of PBI2 to test reproducibility.

In-situ FTIR experiments were carried out using a Varian 670-IR spectrometer equipped with a ceramic, air-cooled infrared source and a cooled DLaTGS detector. The Specac reflectance accessory with an environmental cell (see fig. 1) allows IR spectra to be collected under controlled atmosphere from room temperature to 800 ^oC and pressures from vacuum to 34 atm. The IR beam is incident on the sample in the cell at angles from 20° to 76° with respect to the horizontal plane, via a ZnSe window.

The relative humidity was controlled by passing N_2 through a jacketed Dreschel bottle containing saturated aqueous (H_2O or D_2O) NaCl (200 cm^3). The temperature of the Dreschel was maintained constant between (4 – 40 ^oC) via a Grant LTC1 Water Recycler. The relative humidity of the N_2 exiting the Dreschel bottle was monitored using a Testo 605-H1 humidity meter.

For "absolute spectra", the PBI-coated Ti disc was placed in the sample attachment and mounted on the central, heated pillar of the chamber, which was then purged with N_2 for approximately 50 minutes. A spectrum (S_S, 250 co-added scans and averaged scans at 4 cm^{-1} resolution, ca. 5

minutes per scanset) was collected and ratioed to a reference spectrum (S_R) collected from the uncoated Ti disc under the same conditions. In the temperature and humidity –dependent experiments, the reference spectrum (S_R, 250 co-added scans and averaged scans at 4 cm^{-1} resolution, ca. 5 minutes per scanset) was collected and a second spectrum taken at the reference point (dry N_2, 25 °C), after which spectra (S_S) were collected with increasing relative humidity or temperature. In both cases, the spectra were ratioed to the reference spectrum according to equation (1):

$$\text{Absorbance, } A = \text{Log}_{10}(S_S/S_R) \quad (1)$$

This data manipulation results in difference spectra in which peaks pointing up, to +(Absorbance), arise from the gain of absorbing species S_S with respect to S_R, and peaks pointing down, to –(Absorbance), to the loss of absorbing species. Spectra taken at higher values of relative humidity were ratioed by subtraction, e.g. $A_{90\%RH} - A_{32\%RH}$; ie. no subtraction factor was employed. In the experiments carried out in N_2 as a function of temperature, the reference spectrum was collected at 25° C, after which the temperature was increased to 175°C and then returned to 25°C. The data were then manipulated as in equation (1) with the reference spectrum (S_R) collected at 25 °C, and S_S the spectra collected at higher temperatures. Only the spectra collected up to 100 °C are presented below.

Results

Absolute spectra

Figure 2(a) shows absolute reflectance spectra (ie using an uncoated Ti disc as the reference) of 4.4 and 7.9 μm thick PBI films (PBI1 & PBI2, respectively) over the range 4000 to 500 cm^{-1}, and fig. 2(b) the same spectra over a restricted range. The frequencies of the various features are presented in table 1, along with those reported by Bouchet and Siebert[15] and Musto et al[19].

The 3620 cm^{-1} band has been attributed to the O-H stretch of free water within the film, which can be absorbed during the exposure to air of dry films[10][14] (PBI is able to absorb up to ca. 15 wt.% H_2O at 100% RH[10][15]), and hence the shoulders near 3620 cm^{-1} on both spectra in fig. 2(a) suggest that "free" water is present. We must be careful with respect to what is meant

by “free” water here, as it is unclear from the literature what form of water is being referred to. Such a high stretching frequency, and narrow bandwith, is generally associated with O-H stretches free from hydrogen bonding[21][22], rather than liquid/bulk water.

The 3145 cm^{-1} (ca. 3200 cm^{-1} in the spectrum of the thicker film) and 3413 cm^{-1} bands have been studied in detail, and there is general agreement with respect to their assignment[8-10][15][17– 19] to the stretching of self-associated and free N-H bonds (unassociated and terminal), respectively. The former are due to hydrogen bonding between PBI chains, as shown in scheme 1.

The breadth of the 3145 cm^{-1} feature is due to the variation in hydrogen-bonded ‘chain length’ [8][17] and the form of the absorptions in the N-H region is highly dependent upon the structure and composition, and in all likelihood, the morphology, of the polymer, as was discussed above. Evidence for the potential variability of the structure/morphology of the PBI between films nominally produced by the same method may be found by comparing figs. 2(a) and (b) to comparable spectra in the literature; this reveals marked variation in the ratio of the intensity of the C=C/C=N band at 1620 cm^{-1} to the 1443 cm^{-1} in-plane benzimidazole ring vibration, suggesting a concomitant wide variation in polymer morphology. Thus, from the figures, it can be seen that the intensity of the 1620 cm^{-1} feature in the spectrum of PBI1 is ca. 56% of the intensity of the 1443 cm^{-1} feature; in the spectrum of PBI2, this same ratio is ca. 79%. In contrast, in all but one of the papers reporting mid-IR data on PBI [5][7-9][15][17-18], the 1620 cm^{-1} band is considerably (5 – 8x) weaker than the 1443 cm^{-1} feature. The exception is the paper by Pu and co-workers[16], where the C=C/C=N band is of comparable intensity to the 1443 cm^{-1} feature. There is also some variability in the frequency of the former. The only clear difference between the study of Pu et al and the other studies is the source of the PBI: Pu *et al* obtained their PBI sample from Aldrich, whereas all the other groups sourced their material from Celanese. The PBI employed in the work reported in this paper was sourced from Between Lizenz, Stuttgart, Germany. Further, as can be seen from fig. 2(b), whilst the features of both films in the range 1000 – 1800 cm^{-1} are of similar intensity, the 800 cm^{-1} band in the spectrum of PBI1 is 2.4x the intensity of that of PBI2, yet the N-H absorptions of PBI2 are ca. 3.2x more intense than those of PBI1. It is not unreasonable to postulate that the structure and morphology of the PBI polymer chains are encoded in the IR spectra, rather as the amide I C=O absorptions contain information about the secondary structure of proteins [23].

As may be seen from fig. 2(b), the 1443 band is accompanied by shoulders near ca. 1410, 1460 and 1480 cm^{-1}; this complex group also appears in the spectra reported by other workers, with the relative intensities of the component peaks varying from group to group, (although the frequencies of the shoulders are generally not specified) see for example [7]. Thus, the variation in the relative intensities and, in some cases, frequencies of the IR bands of undoped PBI across the literature suggests that the IR response of such films is dependent upon their structure and morphology and, most likely, their synthesis method and thus the supplier/source of the polymer. Further, the fact that the relative intensities of the various features change suggests that the IR spectrum of a particular sample is a composite of the IR responses of the component chains of varying length/packing/etc.

The effect of humidity

Figure 3(a) shows spectra collected from PBI1 as a function of relative humidity up to ca. 90% ratioed to the reference spectrum collected in pure, dry N_2. The spectra show a broad gain in intensity across the spectral range from 2600 to 3700 cm^{-1}, ie the range covering absorption by self-associated N-H, with increasing humidity, along with broad gains with maxima between 2000 and 2500 cm^{-1}, and near 716 cm^{-1}, the intensities of which appear to track that of the higher frequency feature.

Figure 3(b) shows the spectrum taken at 32% RH subtracted from that collected at 32% in order to ameliorate the effect of the features due to water vapour, over a restricted spectral range. On replacing the 90% RH atmosphere in the cell by pure, dry N_2, the spectra in figs 3(a) and (b) returned to baseline after 30 minutes, showing that the processes responsible for the changes in the spectra were reversible.

It is clear from figs. 3(a) and (b) that increasing humidity has a marked effect on the IR absorptions of the PBI, presumably due to the incorporation of water in the polymer structure: the key question is then where is the water incorporated? Musto et al[8] state that the spectrum of (undoped) PBI below 2000 cm^{-1} is characterized by narrow peaks attributable to ring vibrations, and the work of Ramondo et al[11] on imidazole and Zelinski and co-workers[13] on benzoimidazole suggest that the disruption of the N-H…..N hydrogen bonding (N-H self-association) by the incorporation of hydrogen-bonded water between the PBI chains (see scheme 2) would be expected to have a significant effect upon these ring vibration absorptions due to the impact on C-N and C-C bond lengths. Scheme 2 is redrawn from the paper by Brooks et

al[10] who studied the uptake of water into dry, undoped PBI using, among other techniques, FTIR and NMR. With respect to the former, unfortunately, the authors only considered the IR spectral range between 2500 cm^{-1} and 3700 cm^{-1}; apart from commenting on seeing an increase in the free water band at 3620 cm^{-1}, they concluded that the data was inconclusive with respect to the formation of H-bonded water. In contrast, the NMR data, rate of water uptake and equilibrium water content vs RH were all interpreted in terms of the incorporation of the water into the polymer matrix without interaction- ie. without H-bonding between water and the PBI chains. However, this conclusion is in direct conflict with the generally-held view that incorporation of water is via hydrogen bonding; see for example [15].

The broad, relatively featureless gain between 2600 and 3700 cm^{-1} in fig. 3(a) suggests the gain of hydrogen bonded N-H….H-O-H with varying degrees of association (hence the breadth). The broad gain feature between ca. 1850 and 2750 cm^{-1} may be attributed to the combination band of bulk water[24]. The broad band centred near 720 cm^{-1} is featureless, but has sharp loss and gain bands superimposed upon it, and may be due to the gain of librational absorptions[25] associated with the incorporated water; however, the intensity of the latter feature seems disproportionately large, and further work is required to clarify its assignment.

Figure 3(b) clearly shows the presence of weak gain and loss features across the spectral range from ca. 1700 to 500 cm^{-1}; however, they are too weak to discern clearly. Thus, fig. 4(a) shows the spectrum in fig. 3(a) collected at 90% RH and also spectra collected at ca. 90% RH at the end of two repeats of the experiment in figs. 3(a) and (b) using films PBI3 & PBI4 which were both ca. 7.9 μm thick (0.9 mg cff 0.5 mg loading of PBI1). The broad gain feature having a maximum between 2000 and 2500 cm^{-1} in fig. 4(a) may again be attributed to the combination band of bulk or liquid water; this, along with the clear gain feature near 1670 cm^{-1} (the exact frequency of which is obscured by the loss feature near 1620 cm^{-1}) lending support to the postulated existence of this form of water in the film.

As may be seen from the figure, the loss and gain features below 2000 cm^{-1} are clear; in fact, the increase in the intensities of these bands is disproportionately large compared to the ca. 80% increase in PBI loading. These features may be seen more clearly in fig. 4(b) which shows the spectral range from 2000 to 500 cm^{-1} and omits the spectrum from PBI1. As can be seen, there are a plethora of sharp features, both gain and loss, which bear little resemblance to the spectrum

in fig. 2(b). Again, the disparity between the intensities of the N-H absorptions relative to the sharp features below 2000 cm^{-1} suggests differences in morphology, although detailed analysis is hindered by the highly structured nature of the absorptions above 2500 cm^{-1}, possibly suggesting that this region is dominated by loss features due to the N-H absorptions superimposed upon which are gain features due to water as the N-H hydrogen-bonded networks are disrupted by the incoming water. In order to test the validity of this theory, the experiment represented by figs. 3 and 4 was repeated using saturated NaCl in D_2O to produce the humid atmosphere, and the results are discussed in the next section.

The effect of D_2O

The effect of D_2O vapour on PBI2 is shown in figs. 5(a) – (c). The figures show the spectrum collected at 90% D_2O RH and the spectrum collected at 90% H_2O RH using PBI4 in figs. 4(a) and (b). Both films were nominally 7.9 μm thick, and the spectra ratioed to reference spectra collected in dry N_2.

Figure 5(a) clearly shows the gain of a broad feature giving a maximum near 2386 cm^{-1} attributable to the O-D stretch[26], and the loss of a well-defined, broad feature having a maximum near 3200 cm^{-1}. A comparison of figs. 2(a) and 5(a) clearly shows that the latter is due to H-bonded N-H moieties and a shoulder near 3413 cm^{-1} due to the "free" N-H stretch. Thus, the absorption due to the gain of the O-H stretch of bulk water is overlain by the N-H loss features in fig. 4(a); by using D_2O instead of water, the gain absorption due to the O-D stretch now appears very clearly, and the loss features due to the N-H bands are now also very clear: hence the use of D_2O rather than H_2O has clearly separated the water features from the changes in the N-H region. This can also be seen from the absence of the gain feature near 1672 cm^{-1} (the precise frequency of which is obscured by the C=C/C=N loss feature) in the spectrum of PBI2 that is present in the spectra of PBI1, 3 and 4, and may be attributed to the H-O-H deformation associated with the O-H stretch of free water. The broad gain feature with a maximum near 720 cm^{-1} in the spectra obtained using H_2O is also absent when D_2O was employed. It is clear from the data in fig. 5(a) that, as well as water being hydrogen bonded between the polymer chains, it is also incorporated as bulk water, presumably in pores in the polymer. It is also clear that the incorporation of hydrogen bonding-free water is relatively minor.

It may be seen from figs. 5(b) and (c) that there are more loss features in the D_2O spectrum than in the H_2O spectrum (although these bands may be attributed to the PBI, see table 1), with most being bipolar, with the bands shifting to lower frequency, suggesting that the uptake of D_2O has perturbed the PBI significantly more than the uptake of H_2O. Given the postulated marked dependence of the ring vibrations on the degree of hydrogen bonding between the PBI chains discussed above, then it does not seem unreasonable to postulate that the uptake of D_2O results in the exchange of the N-H for N-D, with concomitant changes in the IR ring absorptions over and above those observed with water uptake. Thus, in contrast to the conclusions of Brooks and co-workers[10], the uptake of water by PBI, as well as resulting in regions of 'free' water, also disrupts the N-H…..N hydrogen bonded network due to the formation of hydrogen-bonded water as in scheme 2.

The effect of temperature

Figure 6(a) shows the effect of heating PBI4 to 100 °C in dry N_2. This experiment was carried out prior to that depicted in figs. 4(a) and (b). The film had been exposed to air during the drying process following casting. It is clear that significant water uptake took place during this time; this is not surprising given that the relative humidity in the UK does not fall below 70%. Figure 6(b) shows the 90% RH PBI4 spectrum in fig. 4(a) and that taken at 100 °C in fig. 6(a); from the figures, it is clear that the two spectra are essentially mirror images, as would be expected if water uptake was reversible.

Conclusions

The absorption of water from the atmosphere by freshly-cast films of PBI is appreciable and relatively rapid. The two primary models of water uptake are either: (1) incorporation without disruption of the interchain hydrogen bonding, as bulk water in pores or as hydrogen bonding-free water or (2) incorporation of water between the polymer chains with the formation of hydrogen bonds and consequent disruption of the interchain hydrogen bonds. Our data clearly show that all of these processes take place: some small incorporation of "free" water, as well as more significant incorporation of bulk or liquid water, and also clear and marked disruption of the interchain, N-H….H hydrogen bonds due to the insertion of water between the chains with the formation of hydrogen bonds between these water molecules and the PBI chains.

The structure and morphology of the PBI films appear to vary between samples, even between samples prepared by nominally identical procedures, as evinced by changes in the relative

intensities of various features in the IR spectra. The possible consequence of this is that significant information on the structure of PBI films is encoded in their IR spectra, but further work is required to elucidate this.

Acknowledgements

We should like to thank the EPSRC for funding under the Hydrogen and Fuel Cells Supergen initiative.

This work	**Li et al[15]**	**Musto et al[19]**	**Assignment[19]**
690	701 vs	705 m	Heterocyclic ring vibration
760	760 w		
800	797 vs	801 s	Heterocyclic ring vibration or C-H out-of-plane bend of 3 adjacent H in substituted benzene ring.
850	840 w	846 m	C-H out-of-plane bend of 2 adjacent H in substituted benzene ring.
906	897 m	902 w	C-H out-of-plane bend of single H in substituted benzene ring.
957	943 m		
987		980 w	Benzene ring vibration
1018	1012 w	1011 w	Benzene ring vibration
1172	1170 m		
1230	1230 w	1226 w	In-plane C-H deformation of 2,6-disubstituted benzimidazole
1290	1285 vs	1286 m	Imidazole ring breathing
1366			
1410 sh		1410 m,sh	C-C stretching
1443	1440 vs	1443 vs	In-plane ring vibration characteristic of 2,6-disubstituted benzimidazole
1460 sh			
1480 sh			
1534	1530 s	1534 m	In-plane ring vibration characteristic of 2-substituted benzimidazole
1590	1599 w	1590 m	Ring vibration characteristics of conjugation between benzene and imidazole rings
1620	1621 vs	1612 m	C=C/C=N stretching
3065	3065 m	3063 w	Aromatic C-H stretching
3145	3145 br	3145 br	Self-associated N-H stretching
3413	3410 s	3415 s	Free, non-hydrogen bonded N-H stretching
3620	3620 m		O-H stretch of free water

Table 1. The features observed in the spectra in figs. 2(a) and (b) and those observed by Li et al[6] and Musto et al[19].

References

1. Samms SR, Wasmus S, Savinell RF (1996) J Electrochem Soc 143:1225
2. Kerres J, Ullrich A, Meier F, Haring T (1999) Solid State Ionics 125:243
3. Cassidy PE (1980) Polybenzimidazoles. In: Thermally stable polymers: synthesis and properties. Marcel Dekker, Inc., New York, Sect. 6.10, 6.18-2
4. Hogarth WHJ, Diniz da Costa JC, Lu GQ (2005) J Power Sources 142:223
5. Aili D, Cleemann LN, Li Q, Christensen E, Bjerrum NJ (2012) J. Mater Chem 22:5444
6. Li Q, He R, Gao J, Jensen JO, Bjerrum NJ (2003) J Electrochem Soc 150:A1599
7. Bouchet R, Siebert E (1999) Solid State Ionics 118:287
8. Musto P, Karasz FE, MacKnight WJ (1989) Polymer 30:1012
9. Musto P, Wu L, Karasz FE, MacKnight WJ (1991) Macromol 24:4762
10. Brooks NW, Duckett RA, Rose J, Ward IM, Clements J (1993) Polymer 34:4038.
11. Ramondo F, Bencivenni L, Gustavo P, Domenicano A (1994) Structural Chemistry, 5, pp 1-7.
12. Hofmann K , Imidazole and Its Derivatives, Part I: Interscience: New York, 1953; pp5-25.
13. Zieliński W and Katrusiak (2012) Crystal Growth & Design, 13, pp696-700.
14. Glipa X, Bonnet B, Mula B, Jones DJ , Rozière (1999) J Mater Chem 9:3045
15. Li Q, He R, Berg RW, Hjuler HA, Bjerrum NJ (2004) Solid State Ionics 168:177
16. Pu H, Liu Q, Yang Z (2005) Polymer Eng Sci: 1395
17. Guerra G, Choe S, Williams DJ, Karasz FE, MacKnight WJ (1988) Macromol 21:231
18. Musto P, Wu L, Karasz FE, MacKnight WJ (1991) Polymer 32:3
19. Musto P, Karasz FE, MacKnight WJ (1993) Polymer 34:2934.
20. Boedeker, 2013, Celazole Polybenzimidazole Specifications, [Accessed 8th October 2013], Avaialble from: http://www.boedeker.com/celazole.htm
21. Dreesen, L.; Humbert, C.; Hollander, P.; Mani, A. A.; Ataka, K.; Thiry, P. A.; Peremans, A. *Chemical Physics Letters* 2001, *333*, 327.
22. Berná, A.; Delgado, J. M.; Orts, J. M.; Rodes, A.; Feliu, J. M. *Electrochimica Acta* 2008, *53*, 2309.
23. Barth, A. and Zscherp, C., Quarterly Rev. Biophys., 35 (2002) pp369 – 430.
24. Giguere, P. A. and Harvey, K. B., Can. J. Chem., 34 (1956), pp708-808
25. Keutsch FN, Fellers RS, Brown MG, Viant MR, Petersen PB, Saykally RJ (2001) J. AM. Chem. Soc. 123: 5938.
26. Lappi, S. E., Smith, B. and Franzen, S., Spectrochimica Acta (2004) Part A 60, pp2611–2619

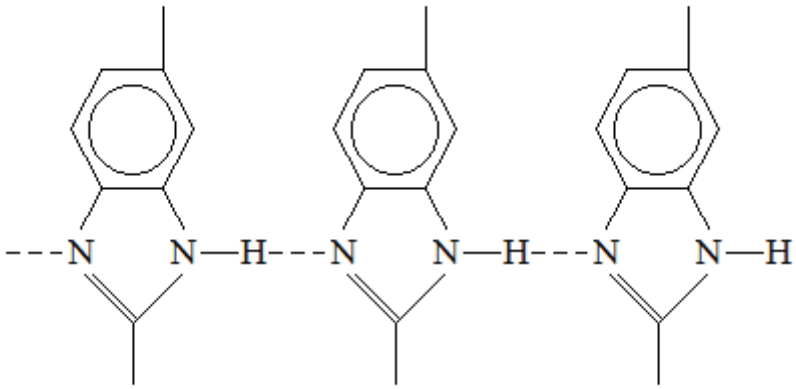

Scheme 1. Self-associated PBI, redrawn from [8]

(I) *(II)*

Scheme 2. Two canonical forms of imidazole, redrawn from [11].

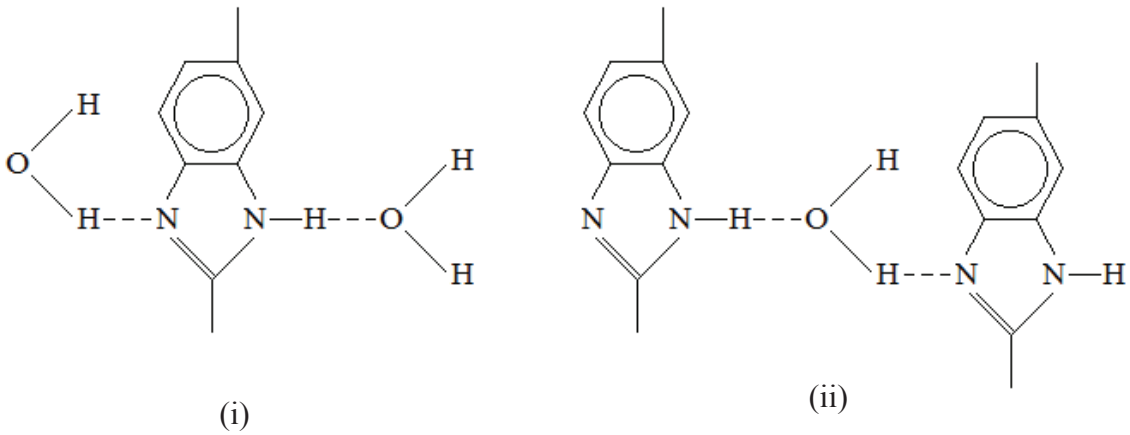

Scheme 3. Uptake of water by PBI: (i) 4 and (ii) 2 water molecules per repeat unit, redrawn from [10].

Figure captions

1. Photograph of the Specac environmental cell.
2. Spectra (250 co-added and averaged scans at 4 cm^{-1} resolution, ca. 5 minutes per scanset) of films (i) PBI1 (4.4 μm) and (ii) PBI2 (7.9 μm); (a) full spectral range, (b) 500 – 2000 cm^{-1}. The films were cast on a polished, 0.95 cm^2 Ti disc. The spectra were ratioed to the reference spectrum of the uncoated disc as according to equation (1).
3. (a) Spectra of film PBI1 collected during an experiment in which the relative humidity (RH) was varied as follows: (i) N_2, (ii) 32%, (iii) 40%, (iv) 50%, (v) 60%, (vi) 70%, (vii) 80% and (viii) 90%. Spectrum (i) was taken to check the stability of the system after the reference spectrum was collected. (b) The spectrum collected at 32% RH in fig. 2(a) subtracted from that taken at 90% RH in the same figure.
4. (a) Spectra collected at 90% RH during repeats of the experiment depicted in fig. 2(a): (i) film PBI3 (7.9 μm) and (ii) PBI4 (7.9 μm) and (iii) the spectrum of PBI1 collected at 90% RH in fig. 2(a). (b) The spectra of (i) PBI3 and (ii) PBI4 in fig. 3(a) over the range 500 – 2000 cm^{-1}.
5. Spectra collected at 90%RH in (i) D_2O (PBI2) and (ii) H_2O (PBI4, spectrum from fig. 3(a)): (a) full spectral range, (b) 1250 – 2000 cm^{-1} and (v) 500 – 1250 cm^{-1}.
6. (a) Spectra collected at (i) 25 °C (second spectrum), (ii) 50 °C and (iii) 100 °C from PBI4. The spectra were ratioed to the reference spectrum taken at 25 °C (first spectrum). The experiment was conducted prior to the humidity experiment depicted in figs. 3(a) and (b). (b) (i) The spectrum of PBI4 collected at 90% RH during the experiment depicted in fig. 3(a) and (ii) that taken at 100 °C in fig. 5(a).

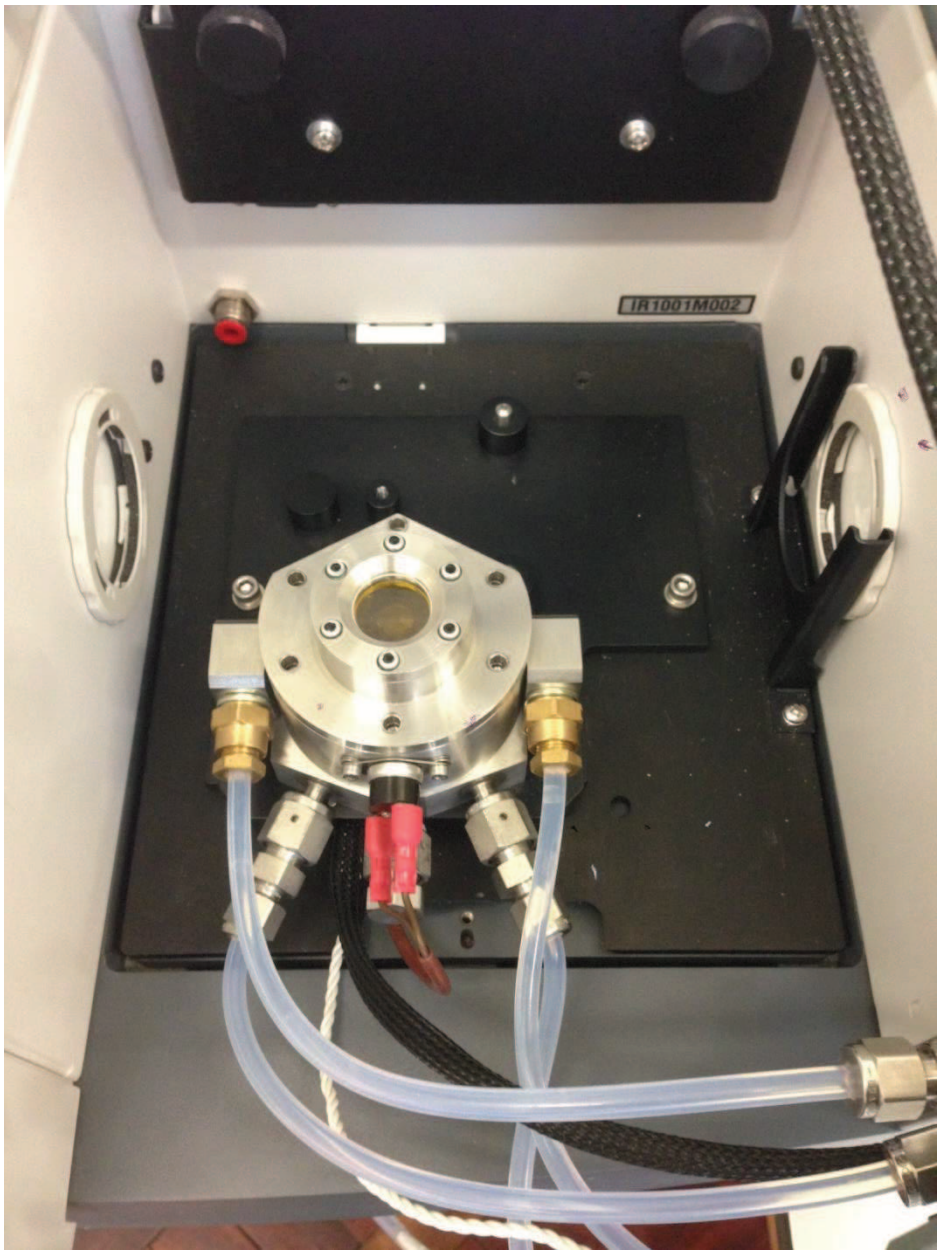

Figure 1

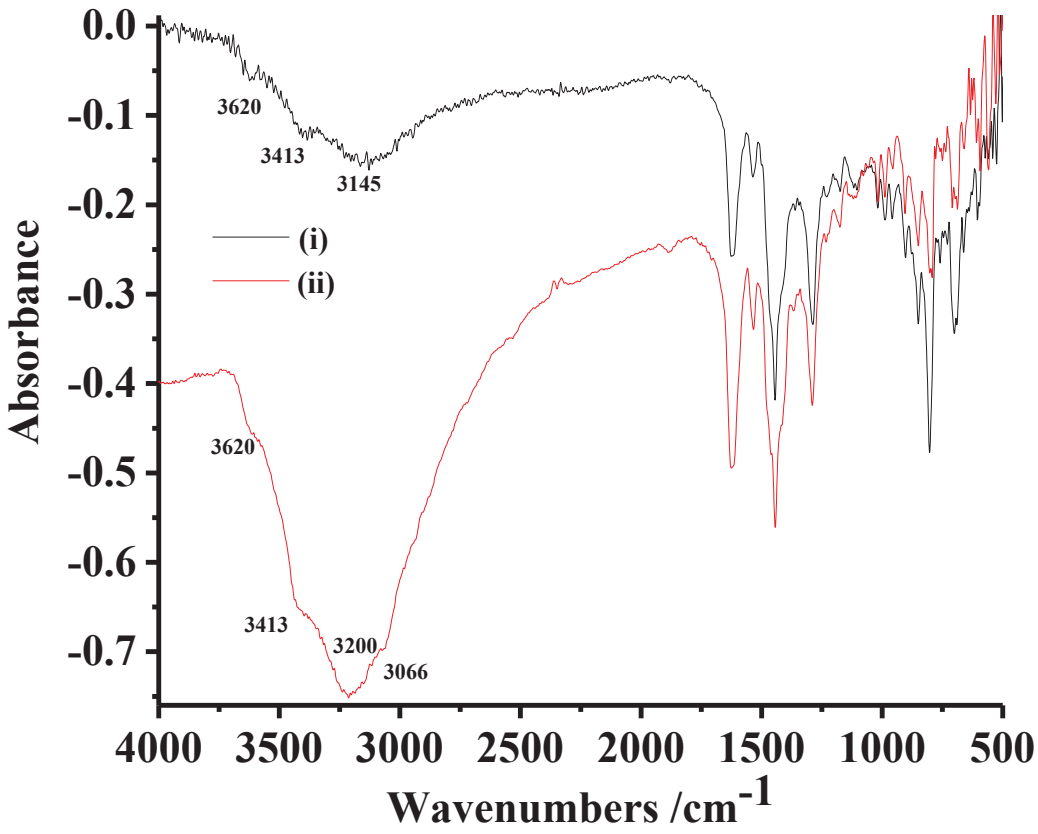
0.0
-0.1
-0.2
-0.3
-0.4
-0.5
-0.6
-0.7
Absorbance
3620
3413
3145
(i)
(ii)
3620
3413
3200
3066
4000
3500
3000
2500
2000
1500
1000
500
Wavenumbers /cm-1

(a)

Figure 2

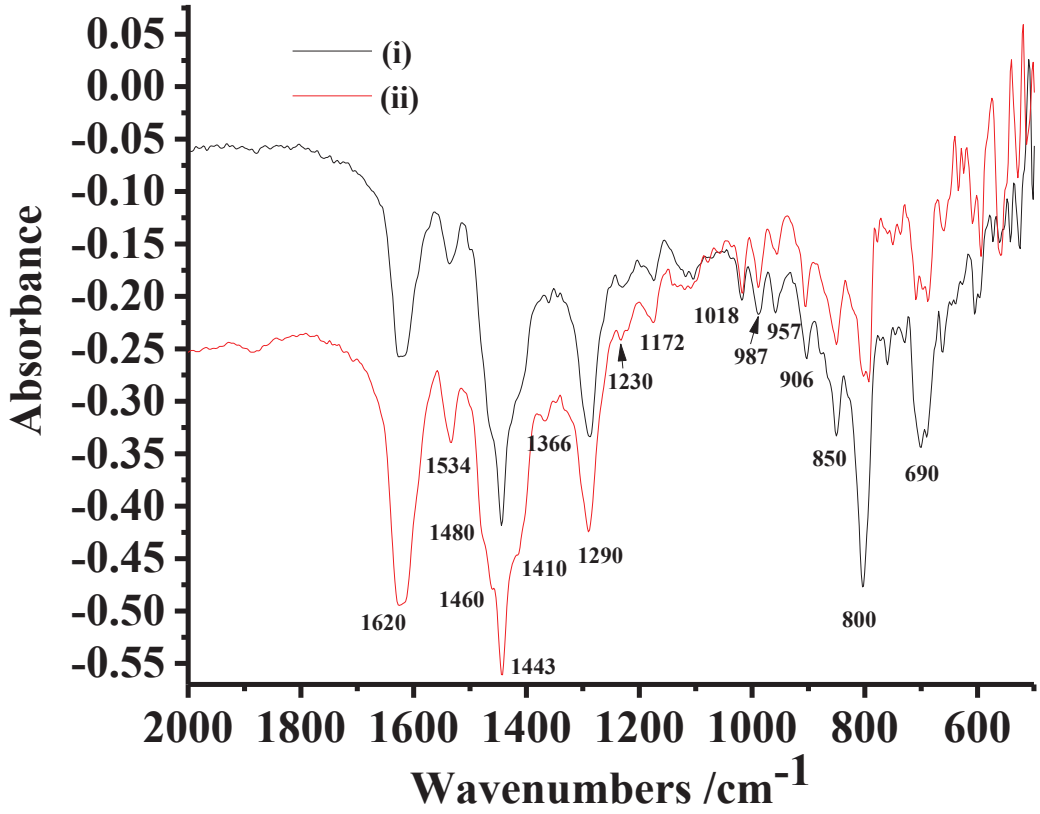
(i)
(ii)
Absorbance
0.05
0.00
-0.05
-0.10
-0.15
-0.20
-0.25
-0.30
-0.35
-0.40
-0.45
-0.50
-0.55
2000 1800 1600 1400 1200 1000 800 600
Wavenumbers /cm-1
1620
1534
1480
1460
1443
1410
1366
1290
1230
1172
1018
987
957
906
850
800
690

(b)

Figure 2

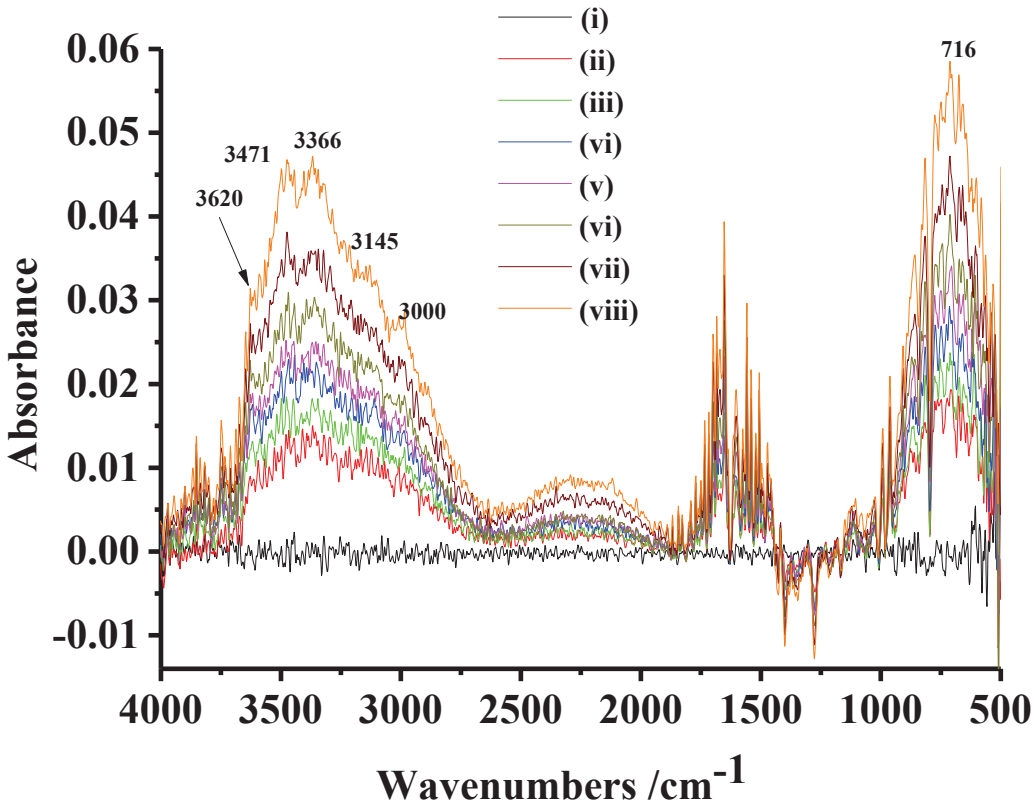
(i)
(ii)
(iii)
(vi)
(v)
(vi)
(vii)
(viii)
3620
3471
3366
3145
3000
716
Absorbance
Wavenumbers /cm-1

(a)

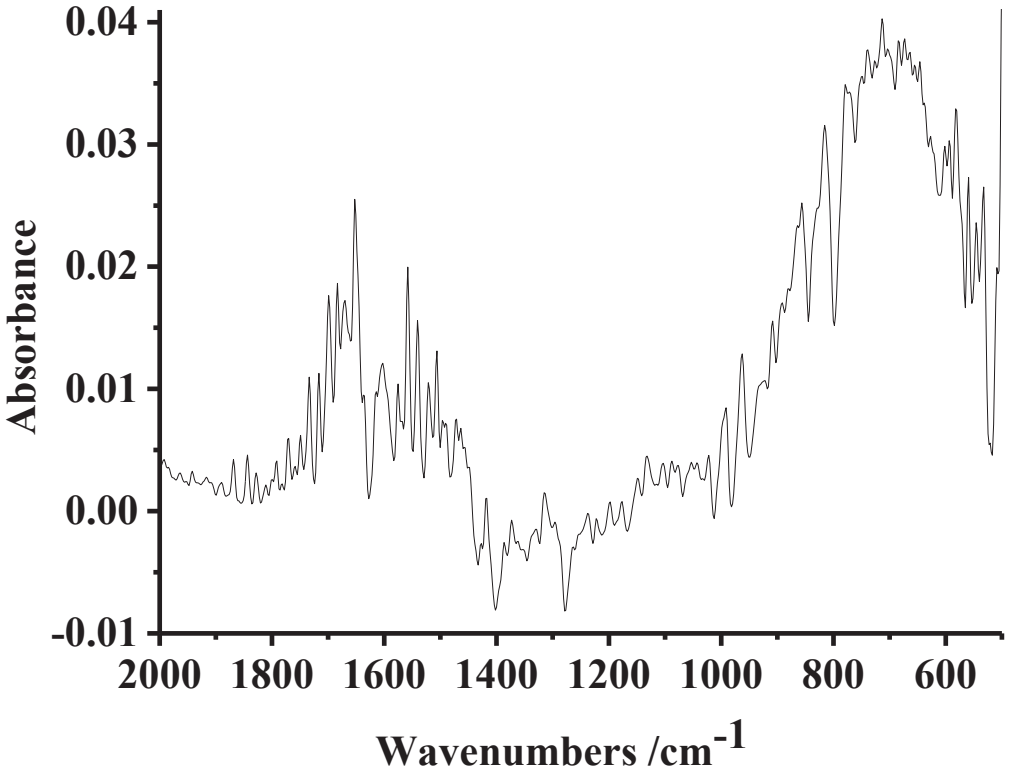
Absorbance
Wavenumbers /cm-1

(b)

Figure 3

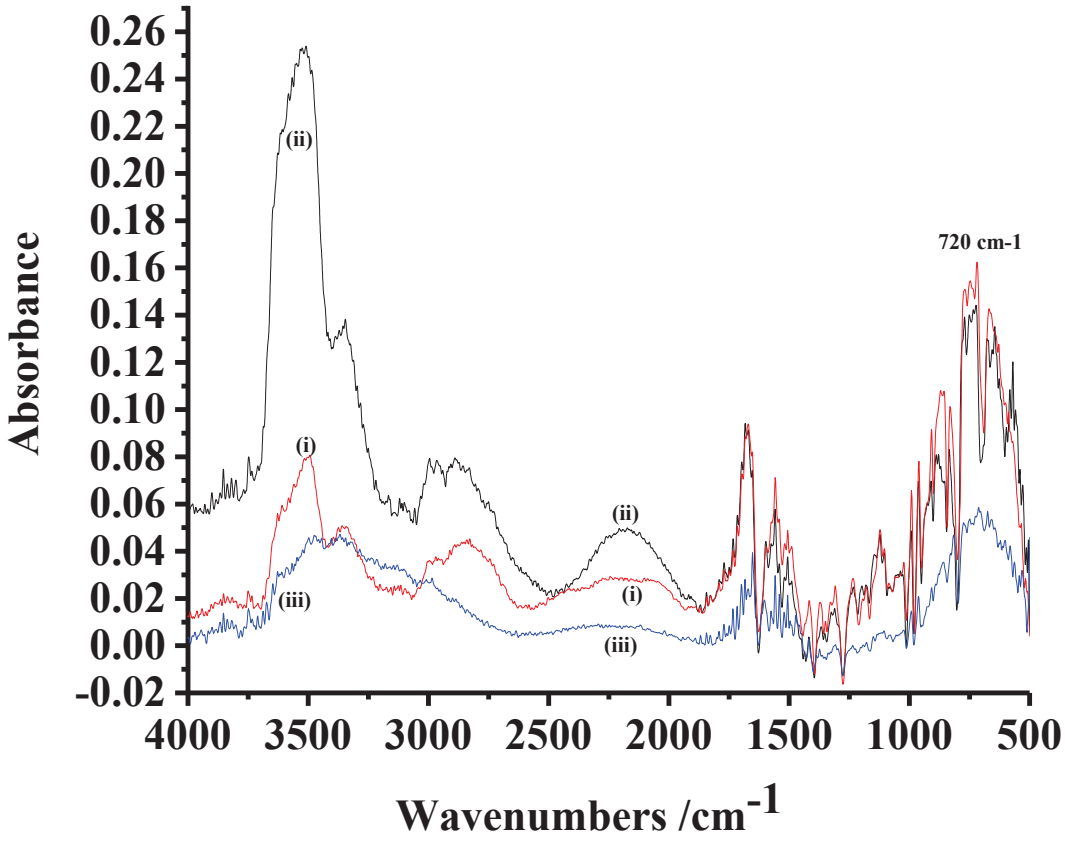
Absorbance
0.26
0.24
0.22
0.20
0.18
0.16
0.14
0.12
0.10
0.08
0.06
0.04
0.02
0.00
-0.02
4000
3500
3000
2500
2000
1500
1000
500
Wavenumbers /cm-1
720 cm-1
(i)
(ii)
(iii)

(a)

Figure 4

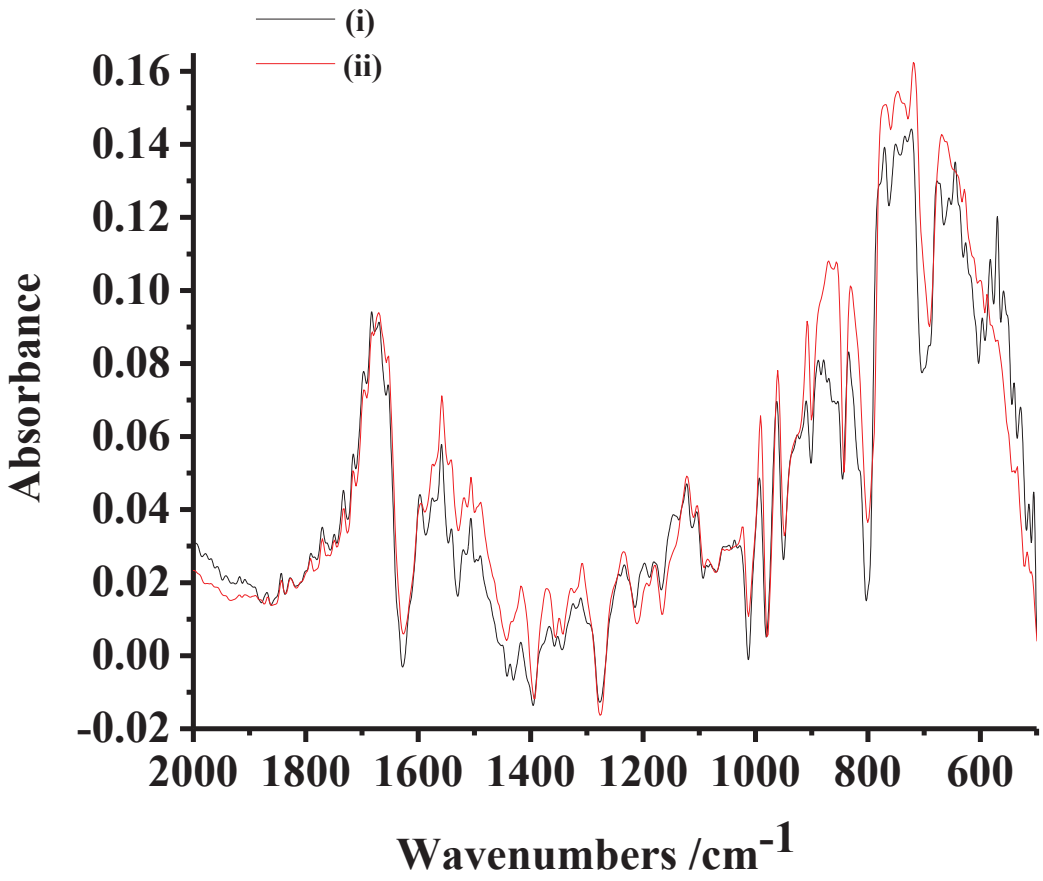
(i)
(ii)
Absorbance
0.16
0.14
0.12
0.10
0.08
0.06
0.04
0.02
0.00
-0.02
2000
1800
1600
1400
1200
1000
800
600
Wavenumbers /cm-1

(b)

Figure 4

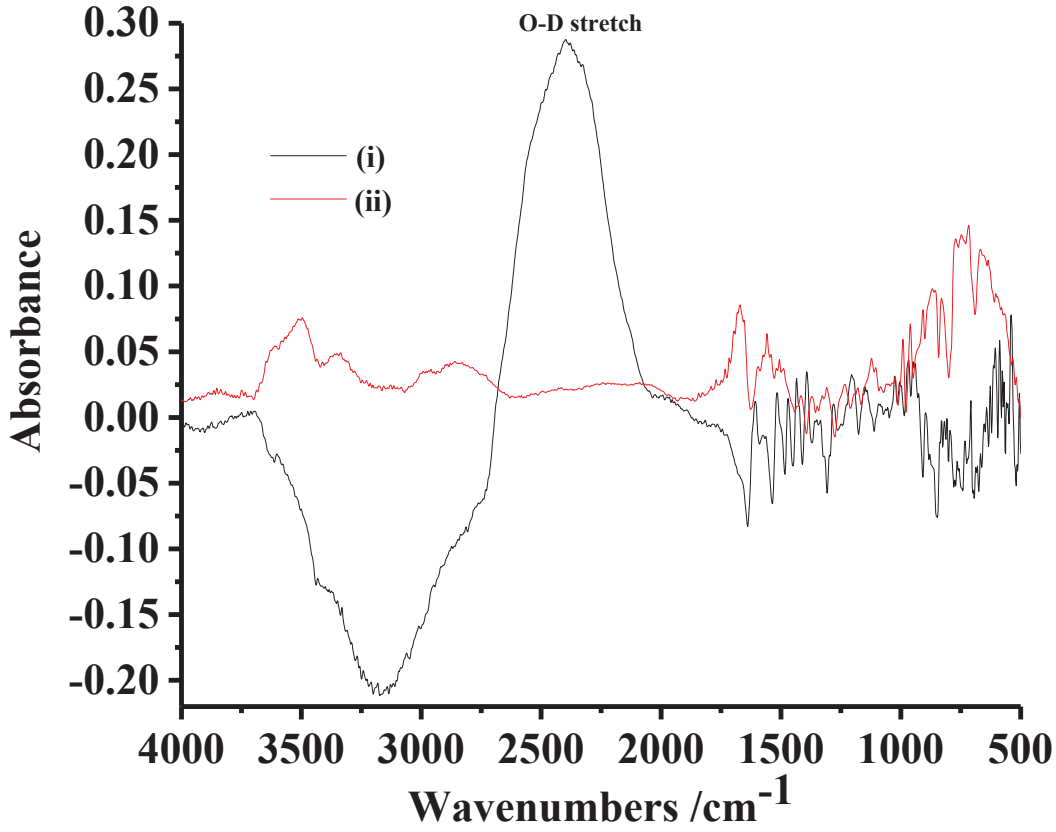
O-D stretch
(i)
(ii)
Absorbance
0.30
0.25
0.20
0.15
0.10
0.05
0.00
-0.05
-0.10
-0.15
-0.20
4000 3500 3000 2500 2000 1500 1000 500
Wavenumbers /cm-1

(a)

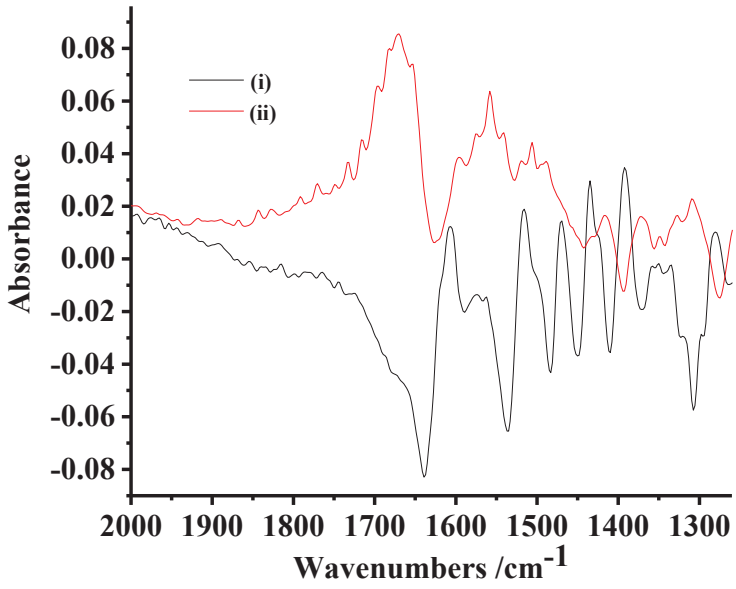
(i)
(ii)
Absorbance
0.08
0.06
0.04
0.02
0.00
-0.02
-0.04
-0.06
-0.08
2000 1900 1800 1700 1600 1500 1400 1300
Wavenumbers /cm-1

(b)

Figure 5

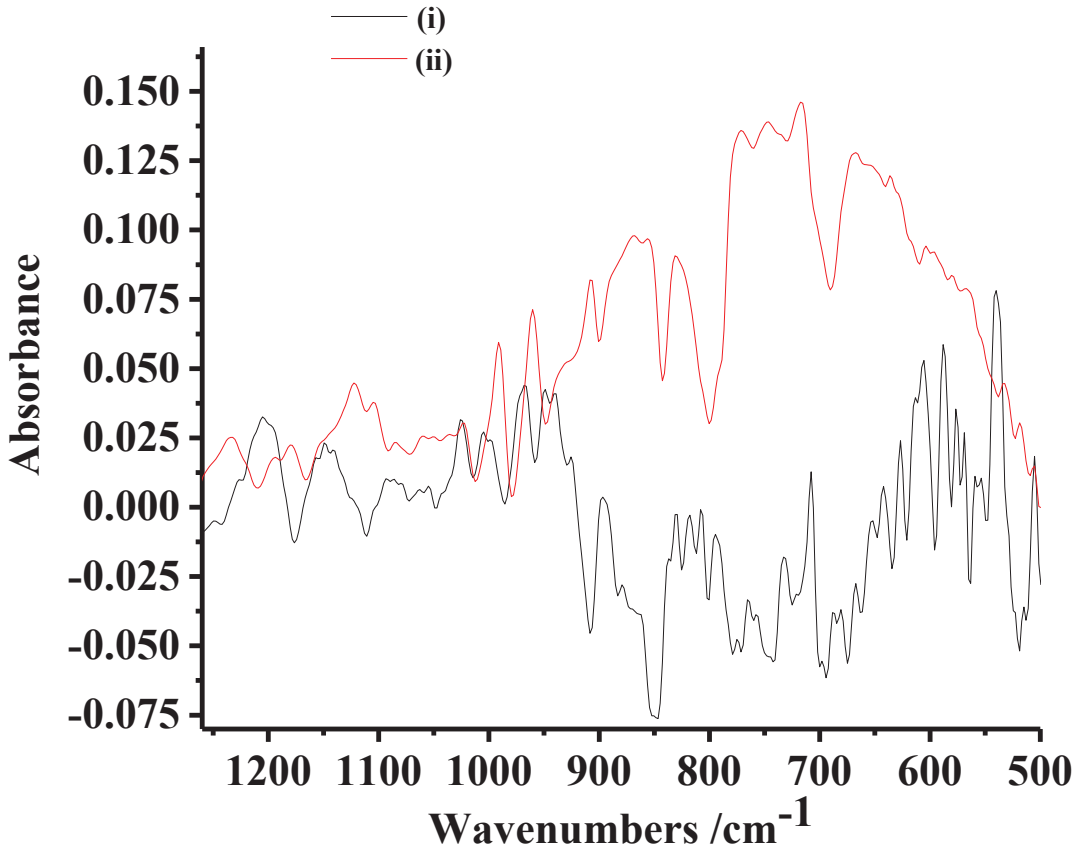
(i)
(ii)
Absorbance
0.150
0.125
0.100
0.075
0.050
0.025
0.000
-0.025
-0.050
-0.075
1200
1100
1000
900
800
700
600
500
Wavenumbers /cm-1

(c)

Figure 5

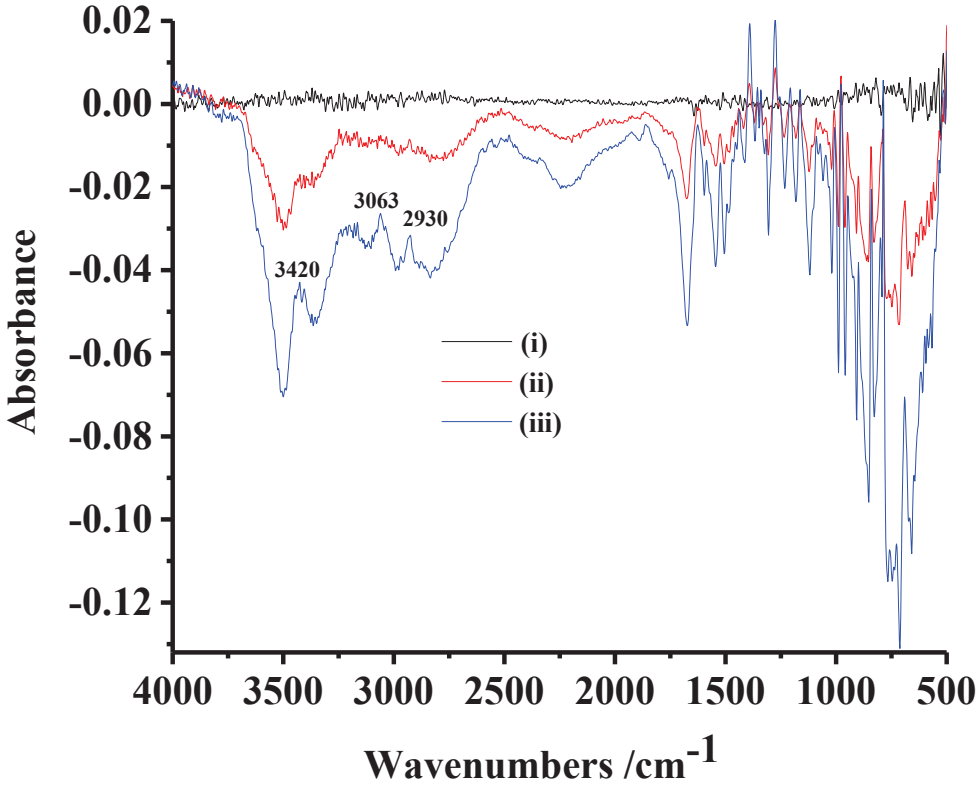
0.02
0.00
-0.02
-0.04
-0.06
-0.08
-0.10
-0.12
Absorbance
3420
3063
2930
(i)
(ii)
(iii)
4000
3500
3000
2500
2000
1500
1000
500
Wavenumbers /cm-1

(a)

Figure 6

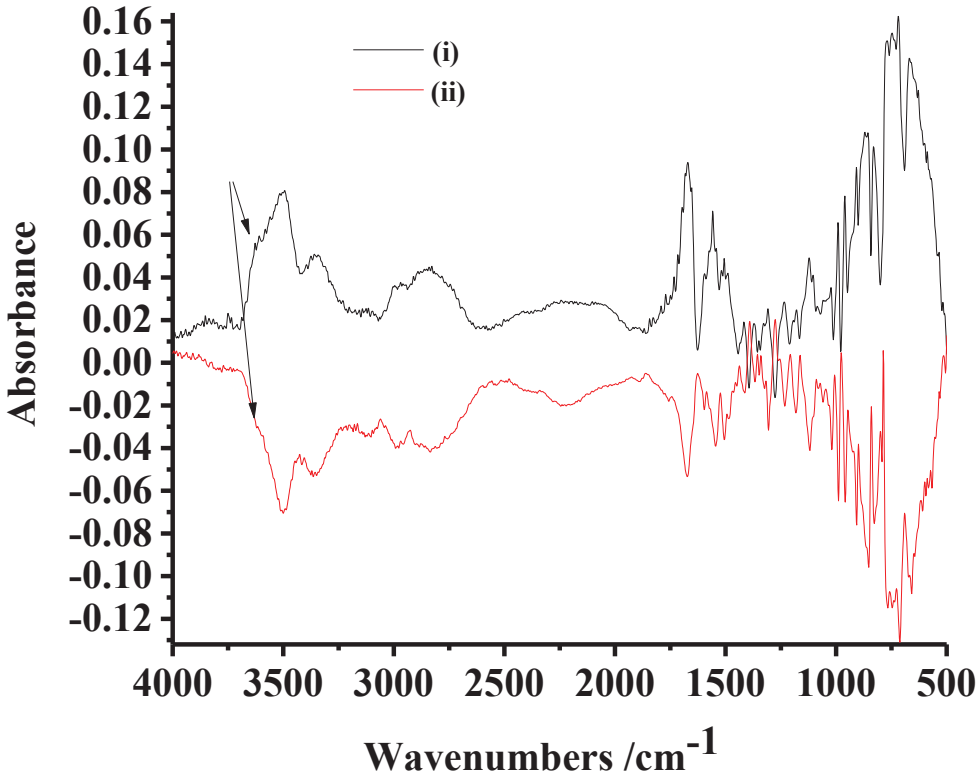
0.16
0.14
0.12
0.10
0.08
0.06
0.04
0.02
0.00
-0.02
-0.04
-0.06
-0.08
-0.10
-0.12
Absorbance
(i)
(ii)
4000
3500
3000
2500
2000
1500
1000
500
Wavenumbers /cm-1

(b)

Figure 6